MEASUREMENTS OF TURBULENCE OVER VORTEX-RIPPLE

by
Masaki Sawamoto
Toshihiko Yamashita
and
Tadashi Kitamura

Tokyo Institute of Technology
Ookayama, Meguro, Tokyo 152, Japan

INTRODUCTION

When a wave propagates over a rippled bed, organized vortices are generated over the leeside slope of crest. They are shedded, collapse and finally supply energy to turbulence in the vicinity of bed. This process plays an important role in the sediment transportation and suspension due to waves. However, quantative measurements of this phenomena have been limited because of some difficulties.

Horikawa and Watanabe(1970) developed the electrolytic transducer and measured the turbulence over a rippled bed. Nakato, Locher, Glover and Kennedy(1977) used a hot-film anemometer controlled by a minicomputer and conducted a phase averaging sampling. One of the authors(1980) tried a phase averaging sampling of velocity field over an artificial ripple by a hot-film anemometer. Du Toit and Sleath(1981) used a He-Ne laser-Doppler anemometer to measure the velocity over artificial and selfformed ripples. Those are the principal contributions in this problem.

One of the difficulties depends on a velocity meter. A hot-film anemometer which is widely used to measure turbulence in an unidirectional flow has some weakness under the circumstances of sediment suspension. Another difficulty lies on a data processing. Because the oscillatory flow turbulence is unsteady process, we can not utilize an analogue data processing technique which is very useful for a steady flow and are forced to handle a large number of digital data.

In the experiments reported here, a laser-Doppler anemometer was introduced in order to overcome a first difficulty. The second one was solved by the combination of a wave-form-recorder-analyser and the desktop computer. The results show the good correlation of the turbulence variation and the movement of shedded vortices. Theoretical considerations on the time averaged turbulence are also presented.

EXPERIMENTAL EQUIPMENT AND CONDITIONS

The wave tank utilized is shown schematically in Fig.1; the test section was 0.4m wide, 0.6m high and 20m long. A 1.8 meter long sand pit was set at the central part of the tank. The same quartz sand, which has a diameter d=0.2mm and density *s=2640 Kg/m3, was used in all cases. An

CASE	WAVE PERID T	WAVE HEIGHT H	DEPTH h	RIPPLE LENGTH Ls	RIPPLE HEIGHT Hs
1	2.25 s	6.90 cm	30 cm	8.55 cm	1.57 cm
2	1.25	6.76	30	4.23	0.88
3	1.75	8.96	30	7.03	1.27
4	1.75	8.52	30	7.18	1.28
5	1.75	6.66	30	6.50	1.12
6	2.25	8.32	30	8.53	1.47
7	1.80	5.15	30	5.75	1.07
8	2.00	6.47	30	7.10	1.46
9	2.00	8.71	30	7.67	1.47
10	2.00	5.15	30	5.43	1.14
11	1.80	8.45	30	6.64	1.22
12	2.60	9.37	30	7.72	1.49
13	2.60	7.63	30	6.74	1.24
14	1.50	7.02	30	5.00	0.97
15	1.40	6.83	30	4.41	0.79

Table   Experimental Conditions
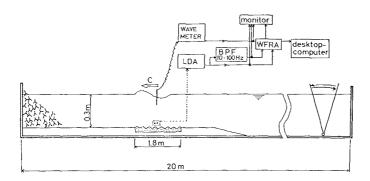

Fig. 1 Sketch of the wave tank.

artificial scratch on the flattened bed made easy to develop a two-
dimensional ripple.
    The experimental wave conditions and the developed ripples are
summerized in Table.   No asymmetrical ripple was observed in the
experimental range listed here.   Fig.2 shows the relation of ripple
length Ls and the horizontal excursion length d_O of water particle.
Cases 12 and 13 locate in the breakoff range and the others in the
equilibrium one where the strong linear relationship are found.
    It was confirmed that the length of the equilibrium ripples has a
good agreement with the empirical equation reported by Homma and
Horikawa (1977).   The ripple height, however, was about 20% larger than
Homma's results.   Yalin and Karahan(1980) also reported the empirical
relation of ripple geometry. Their relation gave a good agreement only
when the propotional constant C,   which they reported 1–1.37, was
modified into 1.6.
    The He–Ne laser–Doppler anemometer(LDA; Nihon Kagaku Kogyo Ltd.)
was used to measure the horizontal velocity under the circumstances of
sediment suspension.   No seeding was need to pick up the frequency-
shifted laser beam.   Under the condition of the sediment concentration
less than one thousand p.p.m., suspended sediment scarcely disturbed the
velocity measurement. The disturbed signals could be easily detected and
discarded.
    Sampling of the output signal from LDA were synchronized with a
wave–meter.   Some phase averaged values were statistically online
analysed and recorded by the wave–form–record–analyser(WFRA;Kikusui
Electronics Co.).   Recorded data were also stored on a magnetic casset
tape and used for further analysis by the desktop computer(HP9835). The
output signal of LDA were filtered by a electrical band–pass–filter in
some cases as mensioned later.

                        DATA PROCESSING METHODS

    Four methods were examined in advance.

i) Direct Phase Averaging Method

    In an oscillatory turbulent flow, the mean velocity and turbulence
should be defined by an ensemble average at a certain phase of wave as
follows

$$U = \frac{1}{n} \sum_{i=1}^{n} u(\omega t + 2\pi i)$$

$$\overline{u'^2} = \frac{1}{n} \sum_{i=1}^{n} [u(\omega t + 2\pi i) - U(\omega t)]^2$$

$$\left.\vphantom{\sum}\right\} \quad (1)$$

where u: instantaneous velocity,   U: phase averaged velocity and u':
turbulence. We refer this averaging PHASE AVERAGING. The phase averaging
can be done by WFRA. This technique may give a good results in case of a
purely oscillatory flow. In a wave field, however, turbulence evaluated
by this method involves two kinds of error.   One is due to wave
randomness.   In a random wave field this is not applicable at all.
Furthermore, whatever good wave maker may be used in the experiment, a
small amount of fluctuation of a wave period and height exist. The
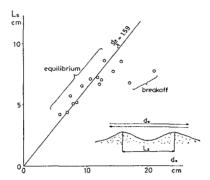
Fig. 2 Relation between the ripple length and the excursion length of water particle.
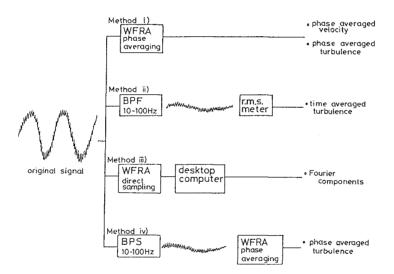

Fig. 3 Data processing methods.

other is due to the imperfect synchronization of sampling. Although the synchronizing signal must be free from any noise or fluctuation, such a situation can not be realized in the experiment. Since turbulence intensity is order of persents of main flow velocity, any fluctuation must be less than one hundredth percent if we want to get an accurate turbulence intensity. Finally, we used this method not to obtain a phase averaged turbulence but only phase averaged main flow velocity.

ii) Electrical Filtering Method

Since phase averaging method is useless in a random wave field, alternative definition of turbulence should be proposed. Turbulence has higher frequency fluctuation than a wave induced periodical velocty variation. So if output signal from LDA was processed by a high pass filter, turbulence velocity fluctuation may be separated. Reading it by a root mean square meter, we obtain long time averaged turbulence intensity as shown in Fig.3. The LDA has inherent noise at higher frequency range than hundreds Hertz, a low pass filter of one hundred Hertz was also used. Cutoff frequency of HPF was determined ten Hertz by trial and error method.

This method seems to be so simple and useful to obtain a set of data at many points. However, it contains a certain amount of error when a turbulence intensity level is low. Because no electrical filter has a sharp cutoff frequency, the high pass filtered signal still has a small fraction of low frequency main flow component which is almost same as or larger than the turbulence. This method was examined at a first stage but finally discarded.

iii) Fourier Expansion Method

The main flow velocity U, which variates in period T, can be expressed by some low frequency terms of the Fourier expansion. Subtracting it from the original variation u, we can obtain an instantaneous turbulent component u' as follows.

$$u' = u - \sum_{i=1}^{N} (a_i \cdot \cos(2i\omega t) + b_i \cdot \sin(2i\omega t)) \tag{2}$$

where
$$a_i = \frac{2}{T} \int_0^T u \cdot \cos(2i\omega t) \, dt \qquad \text{and} \qquad b_i = \frac{2}{T} \int_0^T u \cdot \sin(2i\omega t) \, dt$$

If expansion was carried out in each cycle, this method is applicable to the random wave field. The number of expansion was selected by trial and error. Fig.4 shows the time averaged turbulence intensity calculated by this method. The abscissa is the number of expansion. It shows that the number of expansion should be larger than ten or more which coresponds the cutoff frequency higher than five Hertz.

Although this method make available further complicated analysis, it also forces us to process a large number of digitalized data. So it was used only when a detailed consideration was necessary.

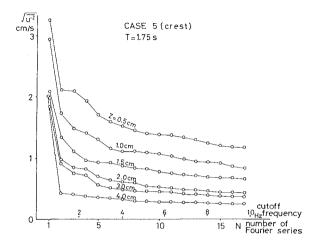iv) Combined Method of Band Pass Filtering and Phase Averaging

Fig. 4 Variation with N of the turbulence intensity evaluated by eq.(2)
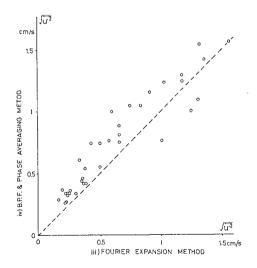

Fig. 5 Comparison of method iii) and iv).

In order to avoid the defects of methods i) and ii), the combined
method of them was developed. The signal processed by the band—pass-
filter was sampled by phase averaging technique. The low frequency
component in the band—pass-filtered signal can be taken away in a
sufficient degree by this method. Almost all turbulence data reported
here were obtained by this method. The comparison of Method iii) and iv)
is shown in Fig.5. The coordinate is the turbulence intensity evaluated
by Method iii) and the abscissa is by Method iv) in which the expansion
number is selected as 17 (cutoff frequency: 10 Hertz).

RESULTS AND CONSIDERATIONS

1) Turbulence Variation and Distribution

Fig.6-1 shows an example of the phase averaged velocity over a
crest. ln the figure, Z is a vertical distance from the crest. The
variation at Z=6 cm , where the bed configuration has no effect on the
velocity variation, is overrapped as a reference variation by broken
lines. Fig.6-2 shows the variations of turbulence intensity and Fig.6-3
does velocity and turbulence distributions.

As shown in the figure, turbulence intensity becomes minimum at the
phase $\omega t = (4/15)\pi$. At this phase, an organized vortex is growing over
the leeside slope, any influence of which is detected at the measuring
section.   After a flow reversion($\omega t = (10/15)\pi$), the vortex moves over
the crest, so the offshoreward velocity is intensified in the vicinity
of bed.   This phenomenon is noticed by a systematic deviation from the
reference velocity variation in Fig.6-1. It is also remarked that the
turbulence   concentrates   in   the   vicinity   of bed. At $\omega t = (18/15)\pi$
another small systematic deviation from the reference velocity is
observed.   It associates the fact that another vortex developed at the
neighbouring ripple passes the measuring section as shown in Fig.6-4
schematically.   Because the vortex passes at higher position, the
turbulence distributes more widely. Although the vortex passes across
the measuring section again at $\omega t = (25/15)\pi$ as shown in Fig.6-4, any
sign is not noticed on velocity or turbulence variation and distribution
because its organized motion has collapsed by this phase. In another
half cycle, almost same phenomenon repeats in the reverse direction.

2) Theoretical Considerations

A turbulence energy budget relation was examined. The turbulence
budget equation is written as

$$\frac{D \overline{q^2}}{D t} = [\text{production}] + [\text{diffusion}] - [\text{dissipation}] \qquad (3)$$

Since the time variation is so complicated, only the time averaged
turbulence intensity is considered. The experimental results including
the visual observation show that the turbulence energy is supplied by
the collapse of vortices in the vicinity of bed and diffused upward by
its diffusivity and that the flow field is almost horizontally uniform
except in the vicinity of bed. Those facts imply the possibility of two
simplified models.

Because the production term does not play any important role except
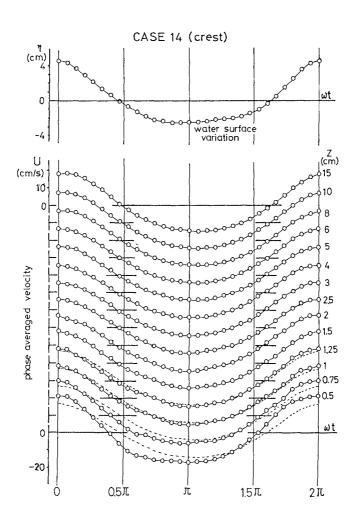in the vicinity of bed,   the diffusion term may balance with the
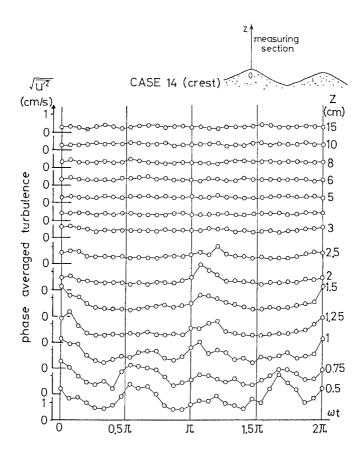
Fig. 6-1 Examples of the phase averaged velocity cycle.

Fig. 6-2 Examples of the phase averaged turbulence variation.

VELOCITY DISTRIBUTION

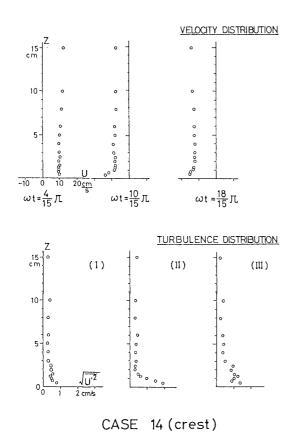TURBULENCE DISTRIBUTION

CASE 14 (crest)

Fig. 6-3   Examples of the phase averaged velocity and turbulence
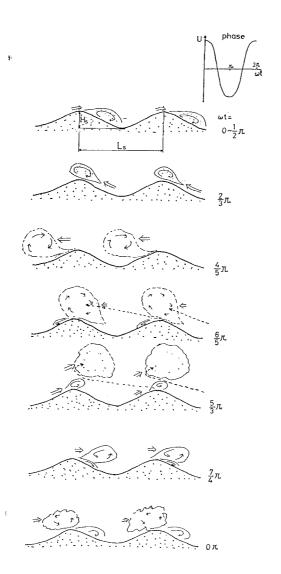   distribution.

Fig. 6-4 Schematic view of the vortex movement.

dissipation term in the upper region shown in Fig.7. If we assume that Prandtl's mixing length hypothesis is also available in this case, we have

$$\frac{\partial}{\partial Z} \, \varepsilon_z \, \frac{\partial \overline{q^2}}{\partial Z} = \frac{A}{L} \, (\overline{q^2})^{\frac{3}{2}} \tag{4}$$

$$\underbrace{\qquad\qquad}_{\text{diffusion}} \quad \underbrace{\qquad\qquad}_{\text{dissipation}}$$

$$\varepsilon_z = B \, (\overline{q^2})^{0.5} \, L \tag{5}$$

where L is the mixing length, $\overline{q^2} = \overline{u'^2} + \overline{v'^2} + \overline{w'^2}$, ε_z is turbulence diffusion coefficient. The value of universal constants A and B are selected as 0.124 and 0.369 by the direct analogy of the unidirectional shear flow. Assuming the mixing length is constant, we obtain

$$\overline{q^2} = \overline{q_0^2} \cdot \exp \left(\frac{1}{L} \sqrt{\frac{2A}{3B}} \, (Z_0 - Z) \right)$$

or
$$\overline{u'^2} = \overline{u_0'^2} \cdot \exp \left(\frac{1}{L} \sqrt{\frac{2A}{3B}} \, (Z_0 - Z) \right) \tag{6}$$

where qo is the reference turbulence intensity at the reference level Zo. Fig.B shows the distribution of time averaged turbulence $\overline{u'^2}$ which must be proposional to $\overline{q_0^2}$. The data fall on the curve predicted by eq.(6). In the theory, the mixing length was selected so that it give the best agreement with experiments, because we have no information about it. The values of mixing length L calculated by this criterion are plotted on Fig.9. It shows a good correlation between the mixing length and the geometrical length scale of ripple in the equilibrium range.

In order to determine the reference turbulence, let's consider the control volume shown in Fig.7. The energy production in a cycle must balance with the energy dissipation in it and the upward diffusion from it. The production may relate with the vortex strength Γ. Dimensional consideration concludes that the production during a cycle is proportional to the square of vortex strength; i.e.

$$[\text{production}] \ = \text{constant} \cdot \Gamma^2$$

The dissipation term is

$$[\text{dissipation}] = \frac{A}{L} \, (\overline{q_0^2})^{1.5} \cdot Ls \cdot T \cdot Z_0$$

The upward diffusion across Zo is

$$[\text{diffusion}] \ = - \, B (\overline{q_0^2})^{1.5} \sqrt{\frac{2A}{3B}} \, Ls \cdot T$$

Assuming Zo propotional to the ripple length Lo,

$$\frac{\Gamma^2}{LsT} = \text{constant} \cdot (\overline{q_0^2})^{1.5} \tag{7}$$

is concluded. Fig.10 shows the relation of reference turbulence intensity and the vortex strength, which was calculated from an
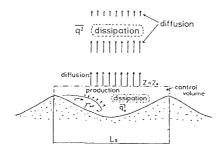
Fig. 7 Schematic relation of turbulence energy budget.

$$(\sqrt{\overline{u'^2}})_m = 1.595 \exp(-0.587 \cdot z)$$
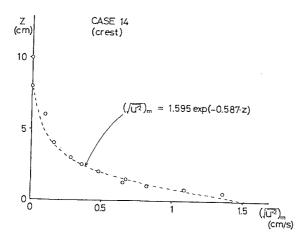
Fig. 8 Example of the time averaged turbulence distribution.
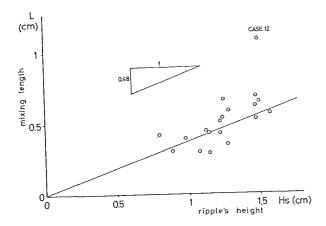
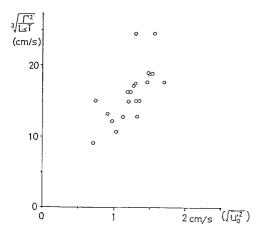Fig. 9   Variation with the ripple height of the mixing length.

Fig. 10   Relation between the vortex strength and the turbulence
          intencity.

accumulation of vorticity flux across the section over the crest by the method proposed by the authors(1980). It shows a good correlation between them.

CONCLUSIONS

Turbulence over rippled beds was measured and the followings were concluded.
1. The variation and distribution of turbulence during a cycle closely relate to the movement of organized vortex shedded from the ripple.
2. The turbulence intensity averaged over a period can be explained through a simplified Prandtl's mixing length model
3. The linear relationship of mixing length and ripple's geometrical length is confirmed.
4. The maximum turbulence intencity which occurs near the bottom relates to the vortex strength.

ACKNOLEDGMENTS

REFERENCES

Du Toit, C. G. and J. F. A. Sleath (1981); Velocity measurements close to rippled beds in oscillatory flow, Jour. of Fluid Mech., Vol.112, pp.71-96.

Homma, M. and K. Horikawa (1962); Suspended sediment due to wave action, Proc. 8th Conf. on Coastal Engg., pp.168-193.

Horikawa, K. and A. Watanabe (1970); Turbulence and sediment concentration due to waves, Proc. 12th Conf. on Coastal Engg., pp.751-765.

Nakato, T., F. A. Locher, J. R. G. Glover and J. F. Kennedy (1977); Wave entrainment of sediment from rippled beds, ASCE, WW1, Vol.103, pp.83-99.

Sawamoto, M. (1980); Flow field over rippled beds induced by wave action, Proc. 3rd Int. Symp. on Stochastic Hydraulics, pp.621-630.

Sawamoto, M., T. Yamashita and T. Kurita (1980); Vortex formation over rippled bed under oscillatory flow, Tech. Rep. No.27, Dept. of Civil Engg., Tokyo Institute of Technology, pp.75-85.

Yalin, M. S. and E. Karahan (1980); On the geometry of ripples due to waves, Proc. 17th Conf. on Coastal Engg.